Electronic Supporting Information for "Shape-selective growth of silver nanoparticles under continuous-flow photochemical conditions"

S. Silvestrini, T. Carofiglio, M. Maggini

S1 – Flow photoreactor for the formation of silver seed nanoparticles

The microfluidic reactor for the nucleation of silver seed nanoparticles consisted in a 4 m long PTFE tube with 0.5 mm internal diameter (from Deutsch&Neumann GmBH) and a total volume 785 µl, coiled around the external jacket of an immersion photoreactor equipped with a high pressure mercury lamp, as shown in figure S1. The tube was connected to a NE300 syringe pump by New Era Pumping Systems Inc. for flow handling. Upon starting the photochemical process, an induction time of a few minutes was observed before the products started to display the typical yellow hue. Such delay was necessary for the depletion of oxygen gas absorbed in the material of the tube, which interfered with the radical reaction leading to the reduction of Ag^{+} to Ag^{0}.

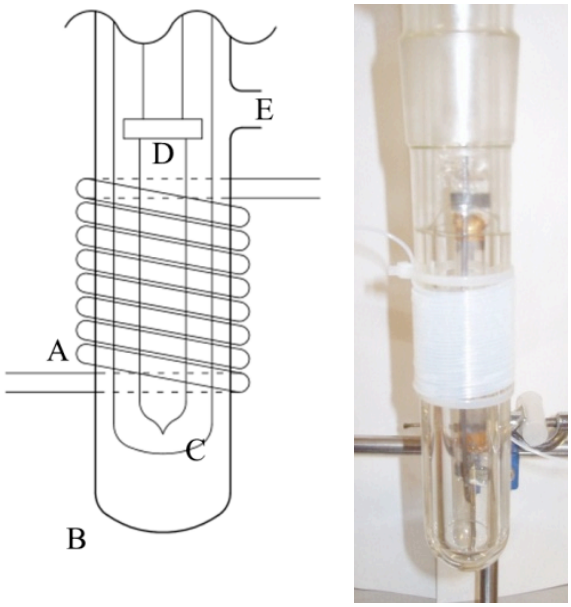

Fig. S1 Microfluidic photoreactor for the seeding of silver nanoparticles. A Teflon tube (A) was coiled around the external jacket of an immersion photoreactor (B). A high pressure mercury lamp (D), masked by the inner jacket (C) provided the illumination, while being cooled by a water flow entering from (E).

S2 – Transmission electron microscopy analysis of silver colloids

A drop of silver NP suspension was deposited on a carbon TEM grid and the liquid was blotted with filter paper to remove the liquid while leaving silver nanoparticles on the grid. The sample was then observed with FEI Tecnai G 12 transmission electron microscope operated at 100 kV. The 8 TEM images presented in figure S2 underwent image analysis to study the size distribution of the seeds. Figure S3 shows the frequency counts of the measured sizes. The analysis was carried out over a total of 1038 particles. Fitting the data with a Gaussian curve yield an average size of 5.9 nm and a standard deviation of 2.9 nm.

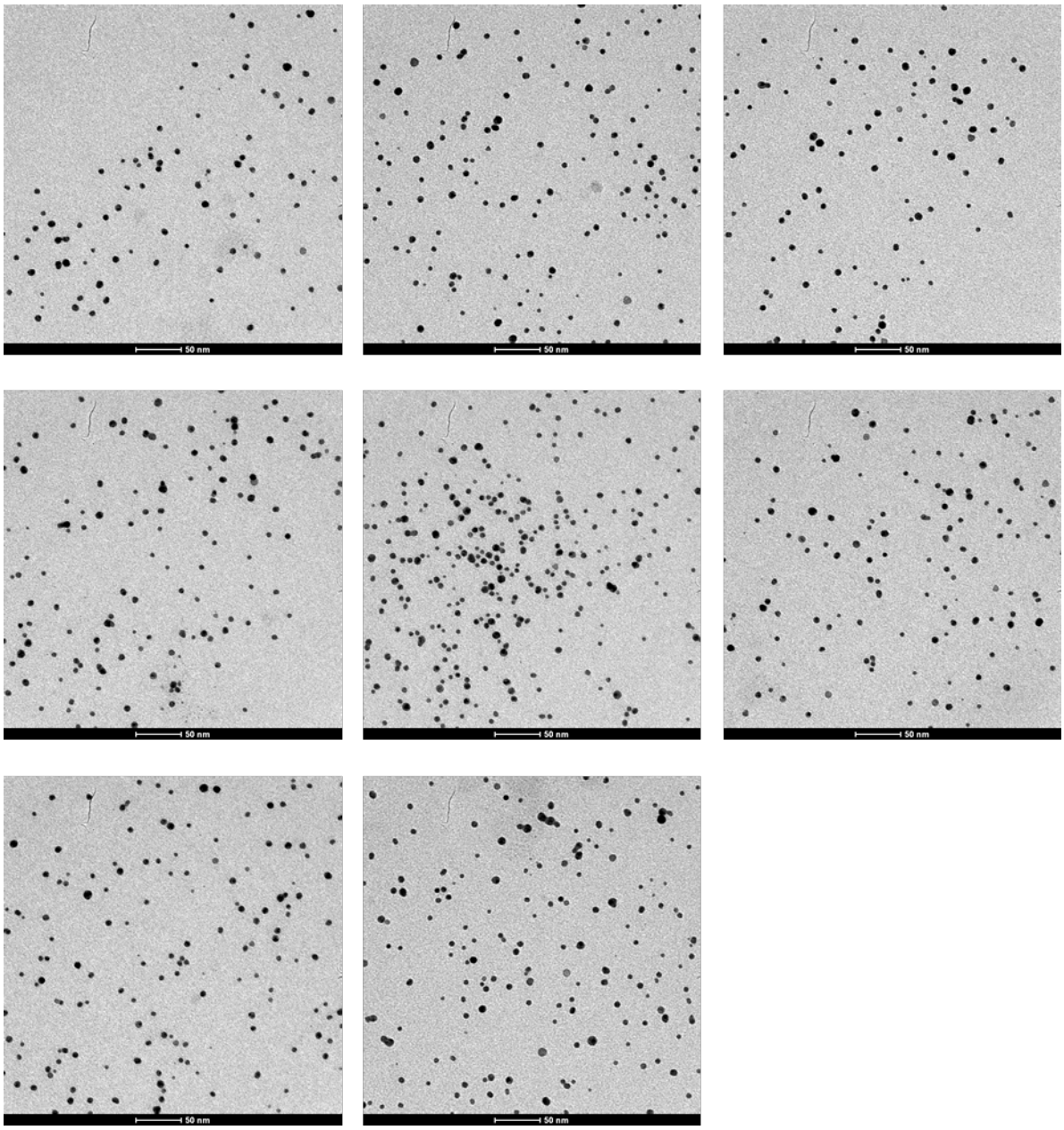

Fig. S2 TEM images of the silver nanoparticles nucleated in the photoreactor.

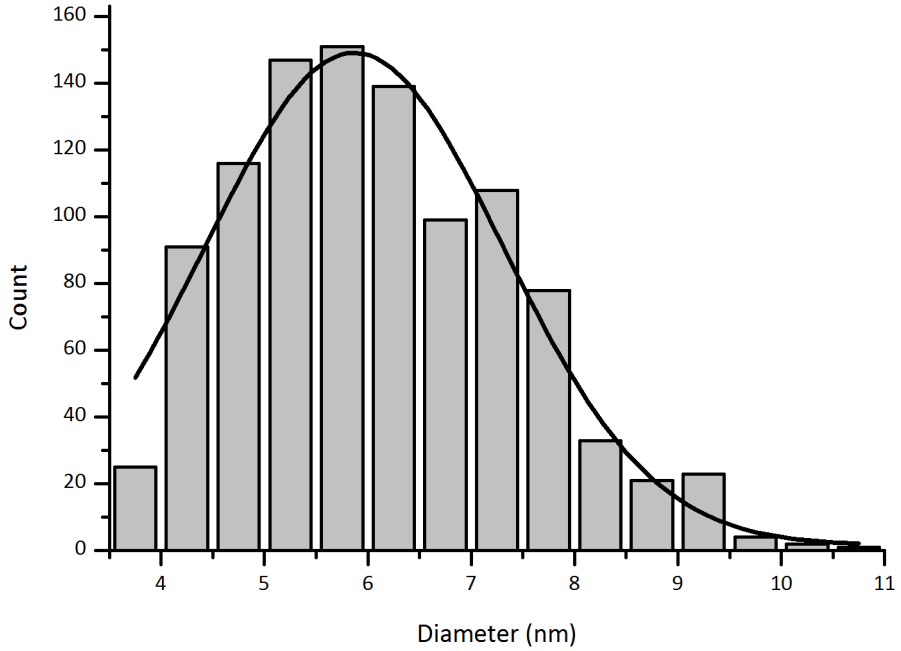

Fig. S3 Frequency count of the size of the NPs from the images reported in figure S2. The solid line represents the Gaussian fitting, yielding an average size of 5.9 nm.

S3 – Silver NP growth according to the photovoltage model

The silver nanoparticles (NPs) that have been described in the paper are crystalline bodies made of metal silver with citrate molecules adsorbed on the surface. They are dispersed in an aqueous medium with dissolved oxygen, so that silver can be oxidized according to the following reaction:

$$2\ Ag^0 + ½\ O_2 + H_2O \rightarrow 2\ Ag^+ + 2\ OH^- \qquad (1)$$

The NPs also exhibit surface plasmons, coherent electron oscillations at the interface between the NP itself and the medium. The oscillation frequencies depend on the shape and the size of the NP, as widely described in the literature (see for instance reference 2 in the article text). Surface plasmons can couple with photons of the correct wavelengths resulting in an hybrid excitation called surface plasmon polariton. For free-standing NPs, the fate of polaritons is propagation until their energy is lost, either by absorption in the metal or by radiative mechanisms. According to the photovoltage mechanism model, on the other hand, these photon-surface plasmon couples are dephased in the presence of citrate molecules, releasing their energy in "hot holes" and causing the photo-oxidation of citrate itself:

$$\text{citrate} \rightarrow \text{acetone-1,3-dicarboxylate} + CO_2 + H^+ + 2\ e^- \qquad (2)$$

The resulting electrons are injected into the metal body, causing a net negative charge (photovoltage) that attracts silver ions from solution, thus promoting the growth of the NP:

$$Ag^+ + e^- \rightarrow Ag^0 \qquad (3)$$

When a monochromatic light is used to irradiate a given sample, those NPs whose surface plasmons resonance frequencies are more closely matched to the incident light, develop a higher potential and therefore grow faster than the other ones thanks to reactions (2) and (3). In addition, only those NPs that absorb light weakly are consumed by reaction (1). In reaction (3), electrons on the nanocrystals must tunnel

across the citrate layer to reduce Ag^+. Citrate is reported to adsorbe more strongly on (111) planes, thus making electron tunneling more difficult and promoting growth along other crystallographic directions.

In all, the process can be thought of an Ostwald ripening phenomenon, driven by the excitation of surface plasmon modes. For in-depth kinetic details on the processes described above, see reference 10 in the main text reference section.

S4 – Fabrication of the polymer microstructured reactor chip

The microreactor (MR) chip was fabricated according to a method developed by Cygan et al for the fabrication of microfluidic channels in NOA resin (by Norland Products) and further developed by Carofiglio et al. with the addition of convenient PTFE tubings as external interfaces (see reference 15 in the main text). We started with the fabrication of the interfaces, as reported in figure S2. Inlet holes (2 mm diameter) were drilled through two glass slides (figure S2a), then a flanged PTFE tubes (2.1 mm od, 1.5 mm id) was fit through the holes in one slide. The slide was set on a beaker, with the tubing facing down and the flanged end on the up side. Pieces of smaller PTFE tubings (1.6 mm, 0.5 mm id) were inserted in the flanged ends and left sticking out, in order to stop the inlet tubing and provide a guide for the positioning of the second glass slide (figure S2b). A layer of liquid NOA resin was poured on the surface and small squares of filter paper were used as spacers (figure S2c). Using the smaller tubes as guides, the second drilled glass slide was placed on top of the first and the assembly was exposed for 5 minutes to UV irradiation (365 nm wavelength) to cure the resin (figure S2d). The resulting element, which we call the "head" of the device, presented all the inlets as 1.5 mm internal diameter PTFE tubing.

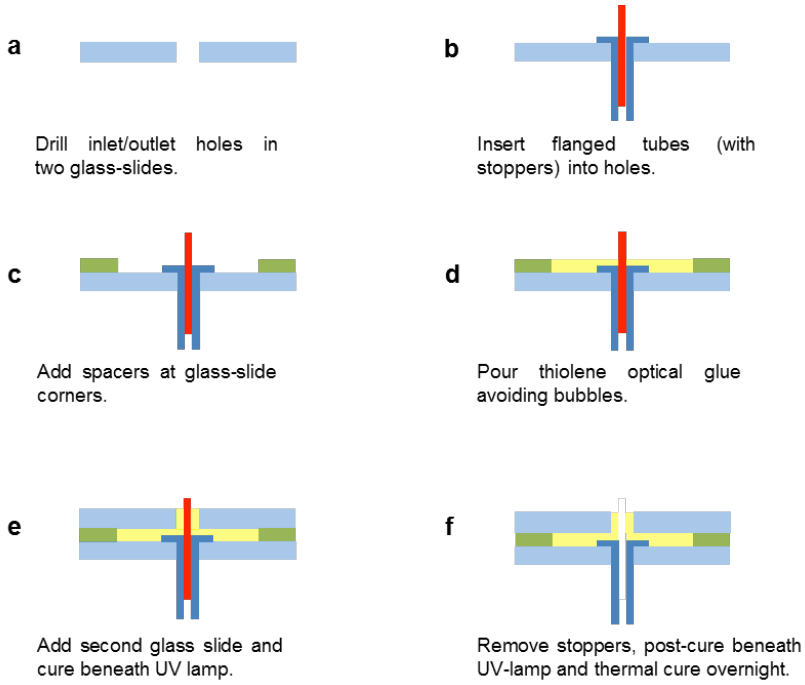

Fig. S4 Fabrication of the external interface (head of the MR).

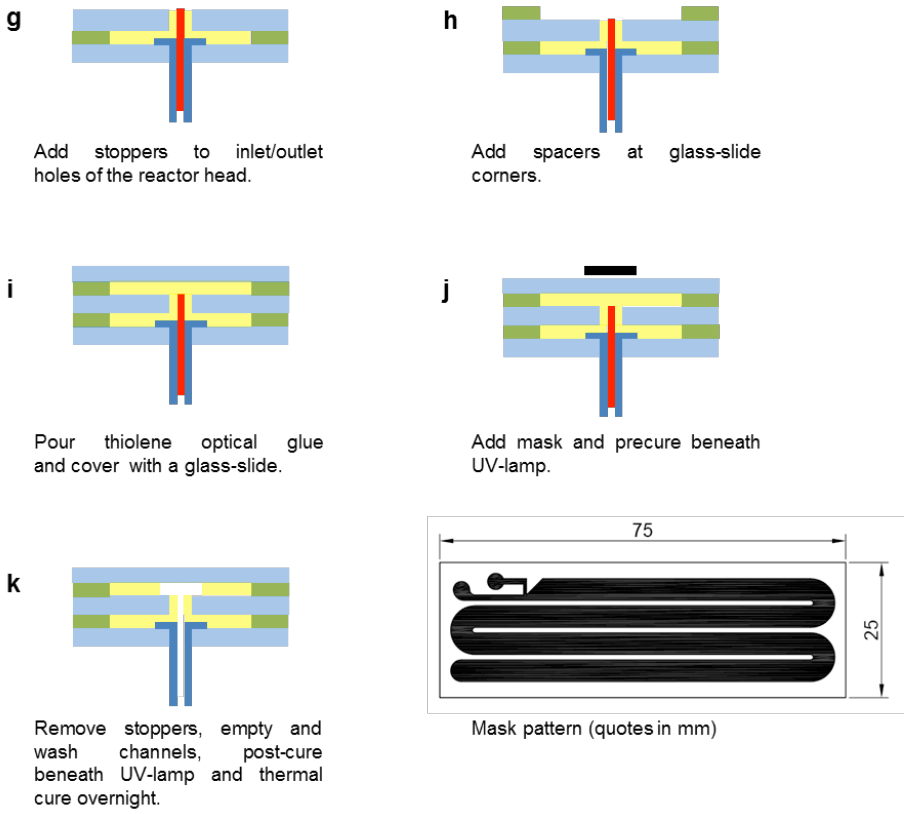

Fig. S5 Fabrication of the channel network.

The channel network was fabricated by soft photolithography on this assembly, as shown in figure S3. After stopping the inlet tubes (figure S3g), another layer of NOA was poured on the surface and more spacers added to set the height of the channels (figure S3h). One last glass slide was set on top of the liquid layer, resting on the filter paper squares (figure S3i). A mask was prepared by printing the desired channel network on transparency paper on a 600 dpi office laser printer and was set over the last glass slide, before irradiating the device for 90 s under the UV lamp (figure S3j). The unexposed, liquid resin was removed by connecting the outlet one by one to a water pump. The channels were then flushed extensively with ethanol in order to remove liquid resin residues, then flushed with nitrogen and exposed to the UV lamp again for 30 min to completely crosslink the resin. Lastly, the device underwent a thermal postcuring treatment at 50 °C overnight (figure S3k).

S5 – Description of LED modules used for sample irradiation

During operation, the reaction vessels (whether cuvettes or microreactors) were illuminated by arrays of 5 high intensity LEDs (C11A1 series, received from Roithner LaserTechnik) mounted on an aluminum heat dissipator as pictured in figure S4. In this work, LEDs operating at 455, 505 and 627 nm wavelengths were used, each with a 10 nm FWHM a 1 W power consumption.

Fig. S6 Array of 5 LEDs mounted on aluminium heat dissipator.